The 2019 World Congress on
Advances in Structural Engineering and Mechanics (ASEM19)
Jeju Island, Korea, September 17 - 21, 2019

Shaking table test for nonlinear dynamic shear force amplification of RC slender wall

*Sung-Hyun Kim[1)] and Hong-Gun Park[2)]

[1)] *Institute of Construction and Environmental Engineering, Seoul National University,*
[2)] *Department of Architecture and Architectural Engineering, Seoul National University,*
[1)] *jangson@snu.ac.kr*

ABSTRACT

In the seismic design of reinforced concrete slender wall structure using nonlinear time history analysis, story shear force created by earthquake load is amplified much more than design story shear force. In the present study, to investigate the amplification effect of shear force, shaking table test was performed for the reduced wall specimens. The specimens were six story wall structure and test parameter was existence of opening in the wall. Test results show that the base shear force was amplified 1.29 ~ 1.51 times after the flexural yielding of the base wall.

1. INTRODUCTION

To prevent the brittle failure of the wall base under the seismic load, it is important to accurately estimate the demand shear force in the design of the slender RC wall structure. However, due to the dynamic characteristics of the seismic load, it is difficult to accurately estimate the demand shear force, especially in the slender RC wall structure due to the shear force amplification effect, which is the phenomenon that the actual shear force under the seismic load amplifies more than the demand shear force predicted in the elastic design.

The reasons of the shear force amplification effect are as follows. First, the seismic load increases with the increase of deformation until the yielding of the member. Thus, due to the increase of the actual member strength by material over-strength, seismic load increases and the actual shear force is amplified than design demand shear force. The current design code (ACI318-19) addresses the shear force amplification due to the material over-strength by multiplying the over-strength factor Ω to seismic shear force V_E.

However, in addition to the material over-strength, the shear force is more amplified after flexural yielding of the wall base by the dynamic characteristics of the slender RC wall. In general, slender RC wall structure has different dynamic characteristics compared to the ordinary moment frame structure: 1) the 1st modal period is much

---

[1)] Researcher
[2)] Professor

larger than the 2nd modal period (T1/T2 in wall structure = 6 vs in moment frame = 3), 2) the effective mass ratio of higher modes is greater (Meff,2~N / Mtotal in wall structure = 35% vs. in moment frame = 25%). That is, the effect of the higher-order modes is greater in the slender RC wall structure than in the ordinary moment frame structure. When the wall base is yielded by the seismic load, the modal periods is increased by the degradation of the lateral stiffness, which increases higher mode effect while decreasing modal effect of 1st mode. Thus, the actual shear force by seismic load is further amplified after the flexural yielding.

In current Eurocode 8 (EC 8), the nonlinear shear force amplification effect is addressed by method of shear force amplification factor (ε) which is multiplied to design demand shear force (V_E). However, in the Korean design code (KBC 2017), which is very similar to IBC 2012, the shear force amplification effect is not considered. Thus, in the present study, to observe the nonlinear shear force amplification effect, shaking table tests were performed on the scaled six stories wall structure specimens.

2. TEST PLAN

2.1 Design and details of the scaled down test specimen

For the test, 1/12 scale three specimens were prepared. Specimen SW and SWR are solid isolated walls. Specimen CWR is a coupled wall in which two walls were connected by coupling beams, to investigate the effect of the coupling beam on shear force amplification effect. In specimen SW, anchorage bond failure occurred in the vertical reinforcement of ϕ6 re-bars because of the relatively small ribs in the re-bars. For this reason, rocking failure mode occurred before full flexural yielding. To avoid early bond failure, specimen SWR and CWR were strengthened by increasing the thickness of the flange and adding additional re-bars.

Considering the allowable capacity of the shaking table machine (Dimensions = 5 m x 5 m, payload = 600 kN), the test specimens were scaled down to 1:12 of the prototype wall. Further, for simplicity, each of two stories of the prototype wall was simplified to one story in the test specimen. Thus, total number of the stories was six stories.

Fig.1 shows the details of the specimens. The uniaxial compressive strength of the concrete specimens was designed to be 30 MPa and the average value of three cylinder specimen strengths on the day of the test was used (Actual strength = 40 MPa). The yield strength of re-bars was SD300 (f_y = 400 MPa) for ϕ6, SD400 (f_y = 500 MPa) for D10. For the D10 re-bars used as diagonal re-bar in the coupling beam, SD500 (f_y = 650 MPa) was used.

As common details, the dimension of the wall section was 800 mm x 90 mm, the story height was 550 mm and the total number of the story was six. Flange walls were used to prevent the out-of-plane failure due to accidental eccentric load during the shaking table test. The size of the flange wall section was 400 mm x 140 mm. The thickness and the width of the slab was 150 mm and 900 mm, respectively. In the specimen CW, an opening was at the center of the wall and the parallel walls were connected by the coupling beam. The dimension of the opening was 200 mm x 350 mm, and the size of the coupling beam section was 90 mm x 200 mm. In the coupling beam, four HD10 (Grade 500, f_y = 650 MPa) re-bars were used for diagonal re-bars. In the specimens

SWR and CWR, the concrete section was increased by thickness of 60 mm, and two additional D10 re-bars were fixed in the foundation by using chemical anchor.

Fig.1 (e) shows the sectional detail of the specimen SW. 10- ϕ6 bars were used for the vertical re-bars of the web wall ($\rho_{v,w}$ = 0.39 %). In addition, D10 was used for the horizontal re-bar and the spacing was 100 mm (ρ_h = 1.58 %). The boundaries of the wall was confined with the U-shaped D10 re-bars. In the flange wall, two additional ϕ6 bars were used for the vertical re-bars ($\rho_{v,b}$ = 0.35 %). The predicted flexural strength of the wall at the base was $M_{n,base}$ = 83 kN-m.

Fig.1 (e) also shows the sectional detail of the specimen SWR, which was a retrofit of the specimen SW. The boundary element was increase by thickness of 60 mm. Two additional D10 anchored into the foundation of the specimen using the chemical anchor were used for the vertical re-bars ($\rho_{v,b}$ = 0.80 %). To increase bonding action between original structure and increased section, stud bolts were installed on the interface of the wall and the chipping was performed to make the interface of the wall rough. Other details were same to specimen SW. The predicted flexural strength of the wall at the base was $M_{n,base}$ = 123 kN-m.

Fig.1 (d) shows the sectional detail of the specimen CWR. 8-ϕ6 bars were used for the vertical re-bars of the each parallel wall ($\rho_{v,w}$ = 0.70 %). In addition, D10 re-bars with spacing of 100 mm were used for horizontal reinforcement (ρ_h = 1.58 %). The boundaries of the wall was confined with the U-shaped D10 re-bars. The coupling beams of the specimen CWR were designed to be in elastic state during excitation. In the coupling beam, 8-ϕ6 bars were used for the longitudinal re-bars and ϕ6 stirrups with spacing of 50 mm were used. In addition, 4-HD10 bars were used for the diagonal re-bars. Other details for retrofitting were same to specimen SWR. The predicted flexural strength of the wall at the base was $M_{n,base}$ = 185 kN-m.

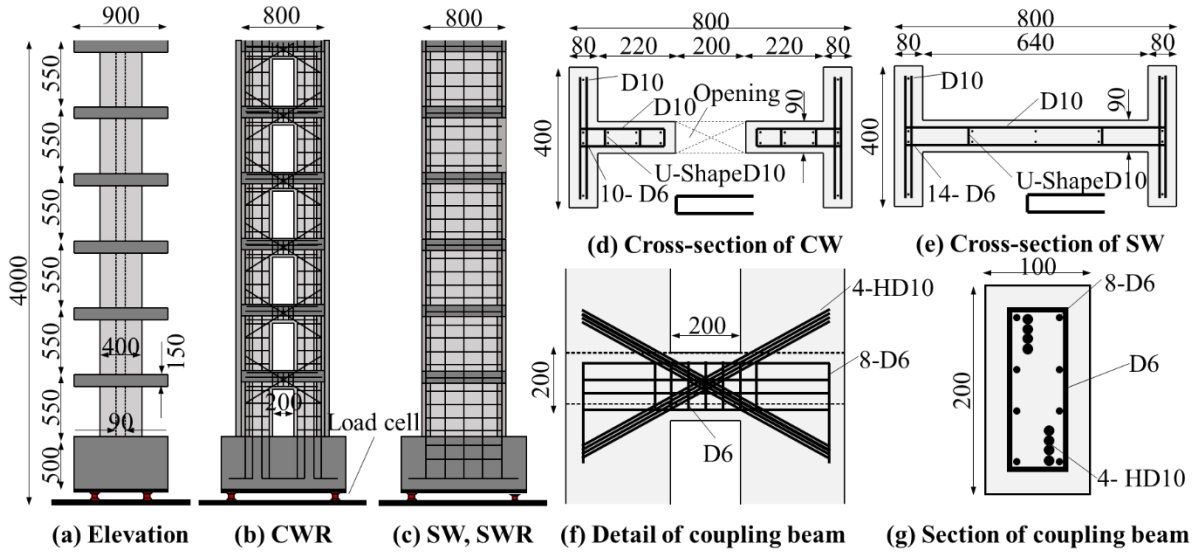

Fig.1 Details of the specimen

2.2 Test Procedure and Instrumentation

Fig.2 shows the test setups and the LVDTs for the measurement of displacement. To simulate the seismic load, using shaking table, the specimen was excited by input

ground motion in the transverse direction. The specimens were simulated only in x-direction. Before every step of excitation of target ground motion, white noise tests were carried out to observe dynamic characteristics of the specimen.

The lateral displacements of the specimen were measured at the center of the each floor slab (Fig.2 (b)). The flexural deformations and the shear deformation were measured in the wall at the first and second floor. The accelerometers were installed at the same height as the locations measuring the floor lateral displacements. In order to measure the reaction force at the foundation, four load cells were installed under the foundation.

For mass of the specimens, steel plates were attached on the each floor to compensate for the difference between the self-weight and the target weight of the specimen following the similitude law. The size of each steel plate was 500 mm x 300 mm x 25 mm. Twenties steel plates were attached on each floor slab excluding the roof. On the roof, six steel plates were attached. To prevent out-of-plane failure during the excitation, the specimen was laterally supported by using a guide frame.

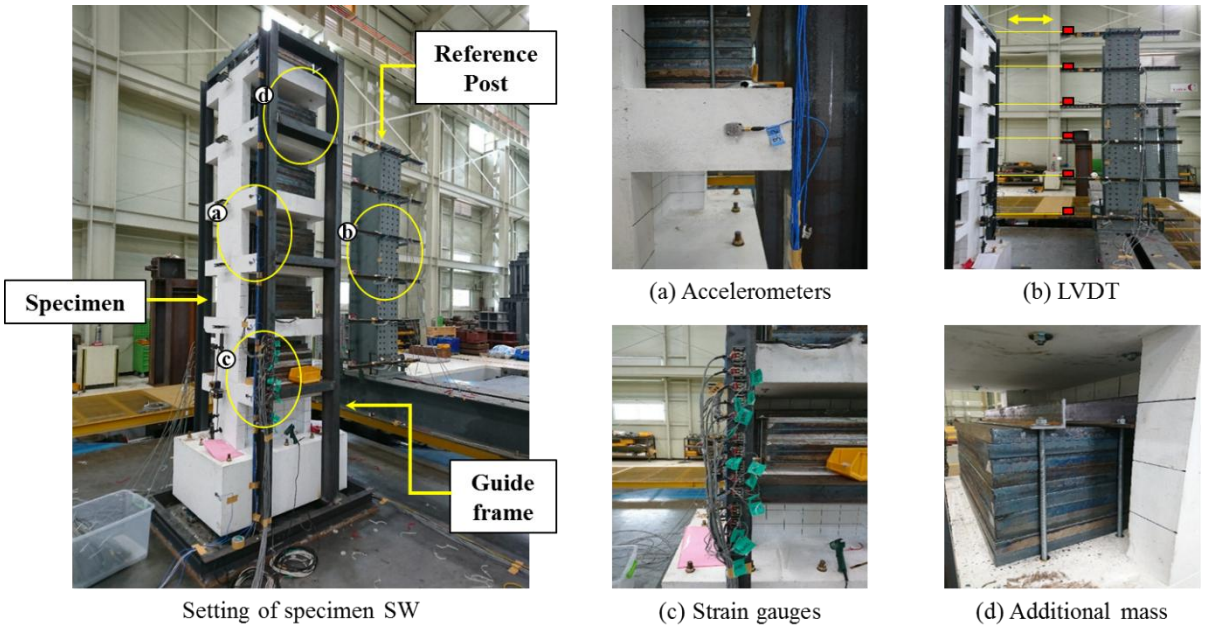

Setting of specimen SW

(a) Accelerometers

(b) LVDT

(c) Strain gauges

(d) Additional mass

Fig.2 Test setup

3. TEST RESULT

3.1 Dynamic characteristics

Fig.3 shows the mode shapes and natural periods from the frequency response function (FRF) analysis using the acceleration data obtained from the white noise tests. The initial natural period in the specimen SW, SWR and CWR was 0.128 sec, 0.086 sec and 0.085 sec, respectively. The measured first and second modal shape of the specimens agreed well with those of the analytical model. As the magnitude of the input ground motion increased, the natural period and damping ratio of the specimens increased due to cracking of the concrete.

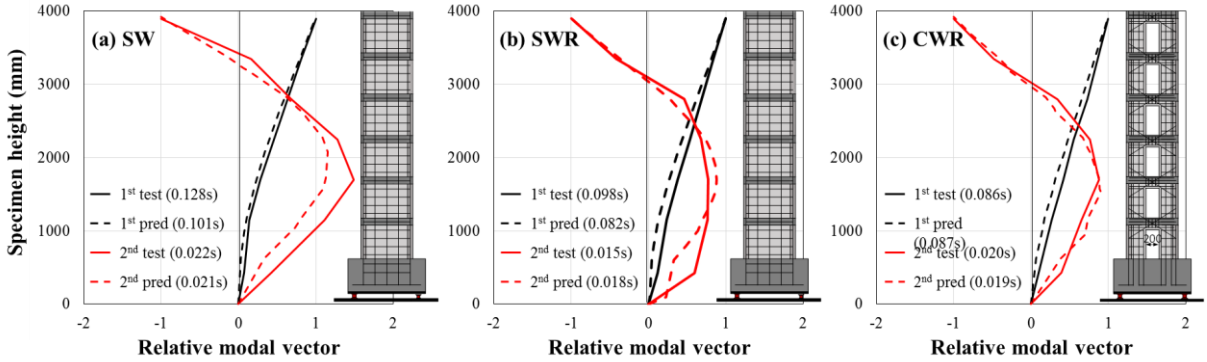

Fig.3 Modal periods and mode shapes

3.2 Failure modes

Fig.4 shows the failure modes of the test specimens. In the specimen SW, bond failure of ϕ6 bars occurred under the input ground motion of PGA = 0.93g. As a result, a macro cracks occur at the interface between the wall and the base slab. After the interface cracking, the specimen showed rocking mode and no damage occurred in the wall. After the final stage of excitation, the wall base was lifted by 1 mm. Shear force amplification effect is caused by inelastic behavior after flexural yielding of the wall. Therefore, such rocking mode is not typical mode in ordinary walls. Thus, SWR and CWR were strengthened with increasing re-bars and thickness of the flange.

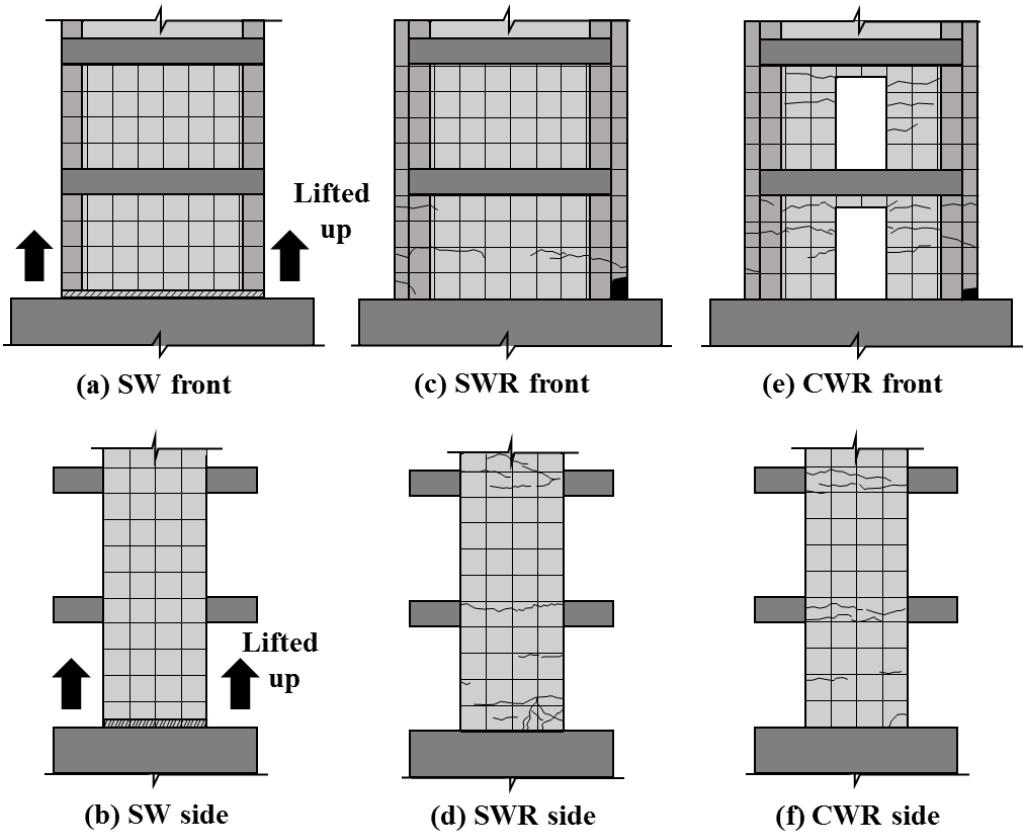

Fig.4 Failure modes

Fig.4 (b) shows the cracking pattern and failure mode of the specimen SWR. The first cracks due to flexural action formed at the excitation of PGA=0.3g. As the magnitude of the input ground motion increased, the horizontal cracks distributed along the wall height. During the final stage of the excitation (PGA = 1.76g), the width of the horizontal tensile cracks at the base increased significantly due to flexural yielding of the wall base. In addition, the cover concrete at the base was crushed. After the end of the excitation program, horizontal cracks penetrating the wall section was observed, which had not appeared in the specimen SW. Damages on the walls in the upper floors were relatively small.

Fig.4 (c) shows the cracking pattern and failure mode of the specimen CWR. The first cracks due to flexural action formed at the excitation of PGA=0.1g. Similar to specimen SWR, the horizontal cracks distributed along the wall height, as the magnitude of the input ground motion increased. At the final stage of the excitation (PGA = 1.31g), flexural yielding of the wall base occurred and the horizontal tension cracks occurred through the wall section. In addition, diagonal cracks occurred around the openings. Crack patterns on the second floor wall were similar to those of the first floor wall. Damages on the walls in the other floors were limited.

3.3 Load-displacement relationships

Fig.5 shows the load-displacement (base overturning moment vs lateral drift ratio) relationships of the test specimens. The base overturning moment was calculated as follows.

$$F_i = m_i a_i \tag{1}$$

$$V_i = \sum_{k=i}^{N} F_k \tag{2}$$

$$M_{test} = \sum_{i=1}^{N} V_i H_i \tag{3}$$

Where M_{test} is the base overturning moment, V_i is the story shear force, H_i is the story height, Fi is the story force, mi is the story mass, ai is the measured story acceleration. The lateral drift ratio was the net lateral displacement of the specimen divided by the net height of the specimen H = 3300 mm. The net lateral displacement (L1-L7) was the difference between the lateral displacement measured at the roof (L7) and the foundation (L1). The net height of the wall H was the height difference between the two measurement points of the lateral displacement.

All the specimens showed peak strength exceeding the nominal flexural strength shown in Table 3. In specimen SW (see Fig. 5 (a)), the peak strength occurred at the lateral drift of 0.49% and -0.47%, respectively. The peak strength M_{test} was +87 kN-m and -81 kN-m in the positive and negative loading directions, respectively, which were 104 % and 96 % of the nominal flexural strength M_n = 84 kN, respectively: M_{test} / M_n = 0.96 ~ 1.04. After the peak strength, the specimen failed in rocking failure mode.

In specimen SWR (see Fig.5 (b)), the peak strength occurred at the lateral drift ratio of +0.40 and -0.30 %, respectively. The peak strength M_{test} was +119 kN-m and -138 kN-m in the positive and negative loading directions, respectively, which were 97 % and

112 % of the nominal flexural strength M_n = 123 kN-m, respectively: M_{test} / M_n = 0.97 ~ 1.12. During the excitation of final input ground motion of PGA = 0.0g, lateral drift increased largely due to flexural yielding of the wall base. After the yielding of the wall, flexural strength was quickly decreased to 48 % of peak flexural strength M_{test}.

In specimen CWR (see Fig.5 (c)), the peak strength occurred at the lateral drift ratio of +0.59 and -0.41 %, respectively. The peak strength M_{test} was +210 kN-m and -177 kN-m in the positive and negative loading directions, respectively, which were 113 % and 96 % of the nominal flexural strength M_n = 185 kN-m, respectively: M_{test} / M_n = 0.96 ~ 1.13. After the excitation of final input ground motion of PGA = 0.0g, flexural yielding of the wall base occurred. After the yielding of the wall, flexural strength reduced to 68 % of peak flexural strength M_{test}.

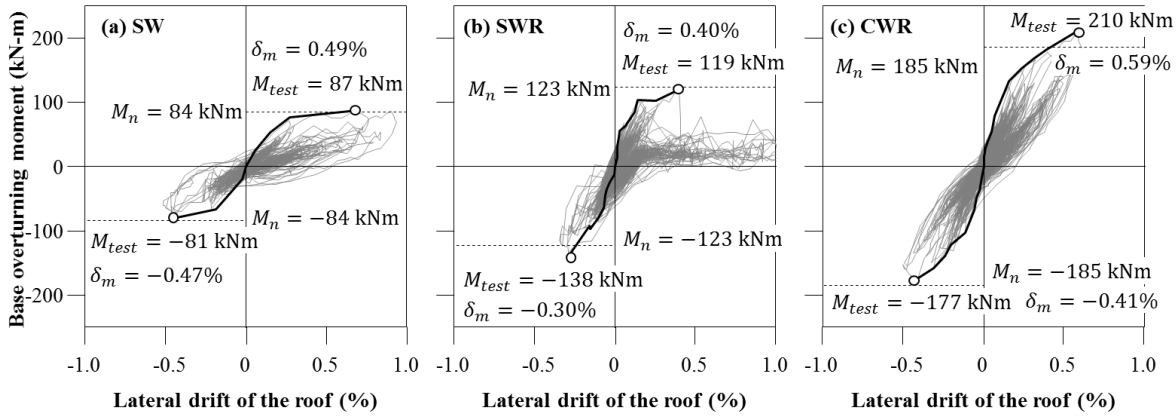

Fig.5 Load-displacement relationships

3.3 Story shear force demand

Fig.6 shows the envelope of the story shear forces and the flexural moments under the input ground motion of maximum peak ground acceleration. In each figure, the vertical axis represents the relative story height to the total height of the specimen. The horizontal axis represents the relative demand force ratio to nominal strength of the wall base. The demand of design force (black dot line) was obtained by the elastic response spectrum analysis. The actual force demand (black solid line) was calculated by the equation (1) ~ (3).

In specimen SW, which failed by rocking failure mode, actual demand of flexural moment in the each floor $M_{test,i}$ reached to design flexural moment M_d (M_{test} / M_d = 0.96 ~ 1.04). However, the tested base shear $V_{test,base}$ was amplified 1.13 and 1.29 times than design base shear force $V_{d,base}$ in the positive and negative loading directions, respectively.

In specimen SWR, which was the retrofit of specimen SW, actual demand of flexural moment in the each floor $M_{test,i}$ reached to design flexural moment M_d (M_{test} / M_d = 0.97 ~ 1.12). The tested base shear $V_{test,base}$ was amplified 1.30 and 1.47 times than design base shear force $V_{d,base}$ in the positive and negative loading directions, respectively. The base shear amplification effect occurred larger in specimen SWR than SW, due to sufficient flexural yielding of the wall base,

In specimen CWR, which had the parallel walls connected with coupling beam, actual demand of flexural moment in the each floor $M_{test,i}$ reached to design flexural moment M_d (M_{test} / M_d = 0.96 ~ 1.13). The tested base shear $V_{test,base}$ was amplified 1.17 and 1.51 times than design base shear force $V_{d,base}$ in the positive and negative loading directions, respectively. The base shear amplification effect in specimen CWR was almost similar with that in specimen SWR, despite of existence of the coupling beam.

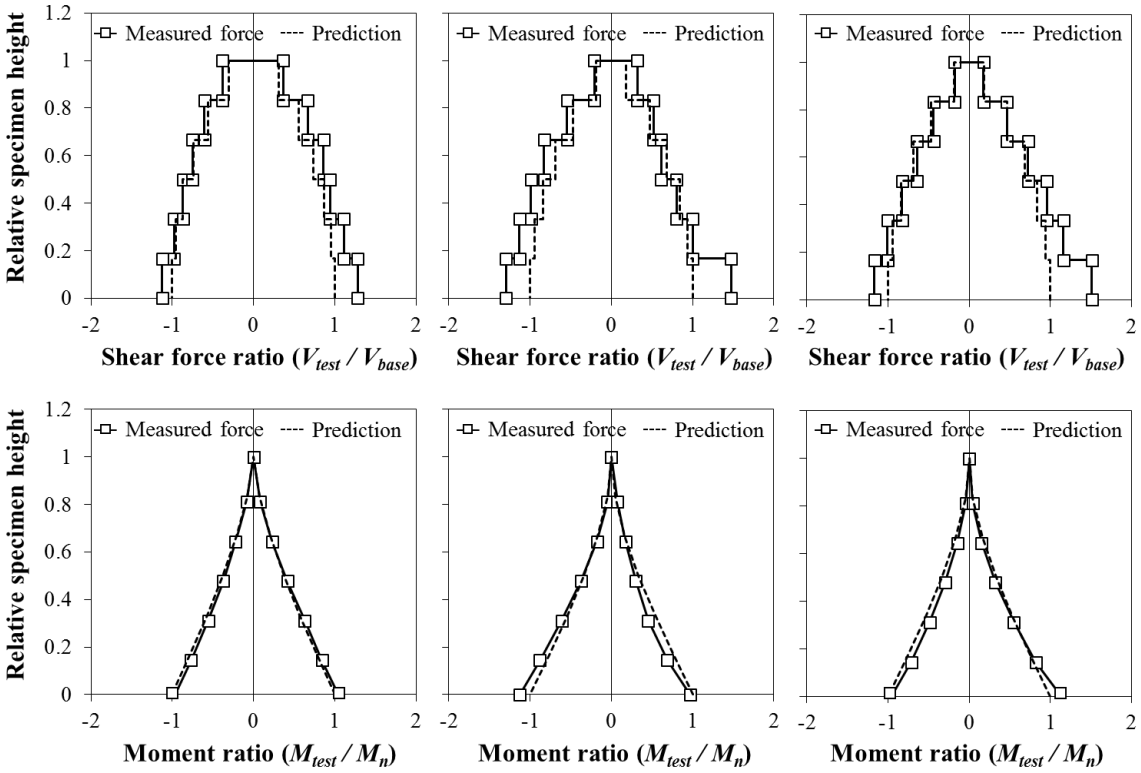

Fig.6 Story shear forces and flexural moments

4. CONCLUSIONS

In this study, to investigate the nonlinear shear amplification effect of RC slender shear wall, shaking table test for scaled down wall specimen was carried out. Test result showed that the base shear force of the specimen was amplified more than design base shear force after the wall base yielded. The range of base shear amplification factor was 1.29 ~ 1.51, which indicates that additional shear reinforcement is required. For future study, test based on test result, numerical analysis models for both the specimens and prototype model are established to perform nonlinear time history analysis. By an analytical parameter study, design factor addressing the nonlinear shear amplification effect is proposed.

REFERENCES

Rutenberg, A, and E Nsieri. (2006) "The Seismic Shear Demand in Ductile Cantilever Wall Systems and the EC8 Provisions." Bulletin of Earthquake Engineering 4, no. 1: